Anode Materials

DOI: 10.1002/anie.201201568

A Highly Cross-Linked Polymeric Binder for High-Performance Silicon Negative Electrodes in Lithium Ion Batteries**

Bonjae Koo, Hyunjung Kim, Younghyun Cho, Kyu Tae Lee, Nam-Soon Choi, and Jaephil Cho**

Electrode designs, which can accommodate severe volume changes (ca. 400%) of silicon anode materials upon lithium insertion, are the main prerequisite for high-performance lithium ion batteries. Among various techniques investigated for this purpose, a robust polymeric binder is a promising means to inhibit mechanical fracture of silicon negative electrodes during cycling.

Lithium ion batteries (LIBs) are one of the most promising energy storage devices owing to their high power and energy densities.[1] For LIBs, silicon is a promising candidate anode material owing to its high theoretical specific capacity of 4200 $mAh\,g^{-1}$ for $Li_{4.4}Si$, low electrochemical potential between 0 and 0.4 V versus Li/Li^+, and small initial irreversible capacity compared with other metal- or alloy-based anode materials.[2] Nevertheless, the practical application of silicon to LIBs is still quite challenging because silicon suffers from severe volume changes (ca. 400%) during Li^+ insertion and extraction processes, which breaks electrical contact between the silicon particles and results in degradation of electrodes and rapid capacity loss.[3] To alleviate volume change, silicon nanoparticles and porous silicon materials have been extensively studied because the smaller particles undergo smaller absolute volume change.[4] The aggregation of silicon particles upon cycling, however, accelerates the degradation of electrodes. Thus, many efforts have focused on the synthesis of silicon–carbon composites to prevent the agglomeration of silicon, resulting in a highly improved cycle performance.[5] Although remarkable improvements in the electrochemical performance of silicon-based anodes have been achieved, electrode deformation and external cell expansion still occur because of the inherent volume change of silicon. This large cell volume change is the main factor limiting the commercialization of silicon-based anode materials.

From a practical point of view, an acceptable degree of volume expansion for the electrodes is about 10%,[6] which is comparable with that of carbonaceous negative electrodes used in current commercial LIBs. To achieve this in a commercially viable silicon-based negative electrode, various approaches have been taken, including the control of electrode porosity[7] and effective distribution of silicon.[8] In particular, attention has been devoted to the development of functional binders that can inhibit the severe volume change.[9] For example, it was reported that good electrochemical performance can be achieved using a polymeric binder in composite electrodes.[10] Recent results have shown that sodium carboxymethyl cellulose (CMC) and poly(acrylic acid) (PAA) binders perform better than poly(vinylidene fluoride) (PVDF) binders in silicon-based electrodes.[11] Beattie et al. reported that silicon-based electrodes with a relatively low silicon content (< 33 wt%) and high binder content (33–56 wt%) can maintain large capacities of about 660 $mAh\,g^{-1}$ for hundreds of cycles.[7c] However, the use of such a large amount of binder and conductive additive leads to a significant reduction in absolute anode capacity. In these composites, the covalent chemical bonds formed by condensation between the free carboxylic acids of the CMC binder and the partially hydrolyzed SiO_2 layer covering the silicon particles prevent the anode from disintegration, which explains the improved cycling stability of silicon–graphite composite anodes.[11c]

Recently, a binder that has a significant positive impact on the electrochemical performance of silicon-based electrodes was reported.[12] Specifically, a high-modulus natural polysaccharide extracted from brown algae was found to yield a remarkably stable battery anode compared with polymers such as PVDF, PAA, and CMC. However, even though this sodium alginate binder assists in building a stable solid electrolyte interphase (SEI),[12] the hydroxy groups remaining after vacuum annealing at 105 °C are a critical problem: they react with PF_5 produced from $LiPF_6$ salt at elevated temperatures,[13] and the resulting phosphorous oxyfluoride (OPF_3) will lead to the decomposition of carbonate solvents, which will in turn lead to rapid degradation of the Si anodes and increased cell impedance.

Herein, we present an innovative thermally cured polymeric binder as a technological solution for lithium ion batteries with silicon-based electrodes. Nanosized silicon powder with a three-dimensionally interconnected network of poly(acrylic acid) and sodium carboxymethyl cellulose as binder exhibits a high reversible capacity of over 2000 $mAh\,g^{-1}$ after 100 cycles at 30 °C and maintains superior capacity of 1500 $mAh\,g^{-1}$ for the high current density of 30 $A\,g^{-1}$ at 60 °C. The cross-linked polymers exhibit high

[*] B. Koo, H. Kim, Y. Cho, Prof. K. T. Lee, Prof. N.-S. Choi, Prof. J. Cho
Interdisciplinary School of Green Energy
Ulsan National Institute of Science and Technology (UNIST)
Ulsan 689-798 (Korea)
E-mail: nschoi@unist.ac.kr
jpcho@unist.ac.kr

[**] This work was supported by the MKE (The Ministry of Knowledge Economy), Korea, under the ITRC (Information Technology Research Center) support program supervised by the NIPA (National IT Industry Promotion Agency) (NIPA-2012-C1090-1200-0002) and by the National Research Foundation of Korea (NRF) grant funded by the Korea Government (MEST) (No. 2011-0027950).

Supporting information for this article is available on the WWW under http://dx.doi.org/10.1002/anie.201201568.

mechanical resistance to strain, and particularly non-recoverable deformation, because the polymer chains are three-dimensionally linked. To the best of our knowledge, this is the first report that shows chemical cross-linking between two different polymers for silicon anodes. This mechanically robust binder showing no swelling in commercialized electrolytes can be expected to prevent any large movement and effectively maintain the silicon–binder bond strength.[12]

The three-dimensionally cross-linked polymeric binder is prepared by a condensation reaction (dehydration) of PAA and CMC (Figure 1). PAA effectively forms the cross-linked structure through the condensation reaction with CMC. The condensation reaction between the carboxylic acid groups of PAA and the hydroxy moieties of CMC occurs at 150 °C under vacuum to afford ester groups by interchain cross-linking. It should be noted that the anhydride can be generated in PAA chains by the dimerization of carboxlic acid (Figure 1 b).[14] Additionally, the free carboxylic acid of PAA and the hydroxy groups of the SiO_2 layer on the silicon surface undergo a condensation reaction to form covalent ester bonds between the binder and the silicon particles. If an interaction occurs in a material, a peak corresponding to

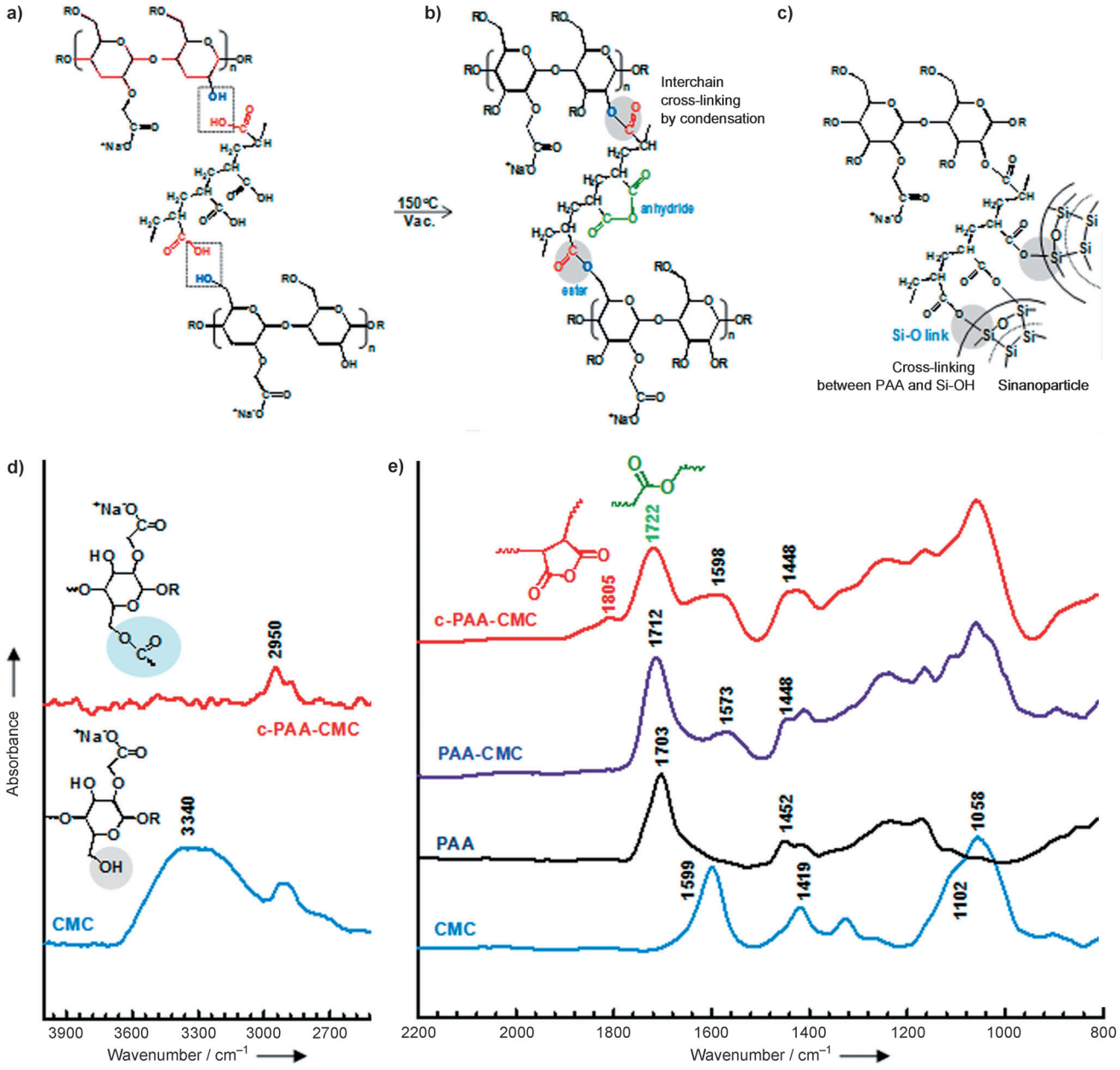

Figure 1. a) Poly(acrylic acid) (PAA) and sodium carboxymethyl cellulose (CMC) before heating. b) Cross-linked binder (c-PAA-CMC) formed by condensation between PAA and CMC. c) Chemical binding between silicon nanoparticles and c-PAA-CMC. The OH moieties of a SiO_2 native layer on the Si surface react with the COOH groups of PAA in cross-linked binder. d),e) Spectroscopic characterization of CMC-PAA heated at 80 °C under atmospheric pressure and of c-CMC-PAA thermally annealed at 150 °C for 2 h under vacuum. The region specific to the carbonyl moieties of the polymers and hydroxy groups of CMC is shown in (d).

a specific functional group in the FTIR spectrum shifts toward either a higher or lower wavenumber or a new peak (or shoulder) appears in the spectrum. The FTIR spectra of polymer films prepared without silicon active materials showed a shift in the position of the C=O stretching band of COOH in PAA from 1703 cm^{-1} to 1722 cm^{-1} that is due to the ester groups (COO) formed by the interchain cross-linking (Figure 1e). It is clearly seen that the broad peak assigned to hydroxy groups at around 3340 cm^{-1} apparently disappears through the condensation reaction between the COOH groups of PAA and the OH groups of CMC (Figure 1d). The characteristic band of the anhydride is located at 1805 cm^{-1} (Figure 1e). Transmission electron microscopy (TEM) showed that the crystalline silicon nanoparticles used in our work had an amorphous SiO_2 layer with a thickness of 5 nm (Supporting Information, Figure S1). In the ^{29}Si magic angle spinning (MAS) NMR spectrum for a silicon composite electrode and silicon nanopowder, the peak corresponding to the OH groups at $\delta = -102$ ppm[15] on the surface of the SiO_2 layer on silicon nanopowder disappeared after heating at 150 °C under vacuum for 2 h. This is because a covalent ester bond forms between the free carboxylic acid groups of PAA-CMC and the OH groups of the silicon nanoparticles by a condensation reaction (Supporting Information, Figure S2). This covalent bond between the c-PAA-CMC binder and silicon nanopowder will effectually restrain any large movement of the silicon nanoparticles. Thus, this could prevent destruction of the electrical network under the large volume change experienced by a silicon composite electrode during cycling. The formation of an efficient network by covalent bonds between binder and nanoparticles has been previously identified as one of the strongest factors governing the electrochemical performances of silicon-based electrodes.[16] Silicon composite anodes with the three-dimensionally interconnected binder (c-PAA-CMC) were found to exhibit a significantly enhanced reversible capacity and a high initial coulombic efficiency (ICE) of 88.2% when compared with anodes incorporating PVDF binder (ICE = 37.9%) during the first cycle (Figure 2a). The low ICE of the silicon anode with PVDF binder is difficult to explain solely by the SEI formation because there is no discernable difference between binders in the potential range between 0.5 to 0.8 V versus Li/Li^+ (Figure 2a). It is known that PVDF binder undergoes plastic deformation in the silicon anodes showing large volume change upon lithium insertion and extraction.[11a] Mechanical disintegration of the silicon electrode

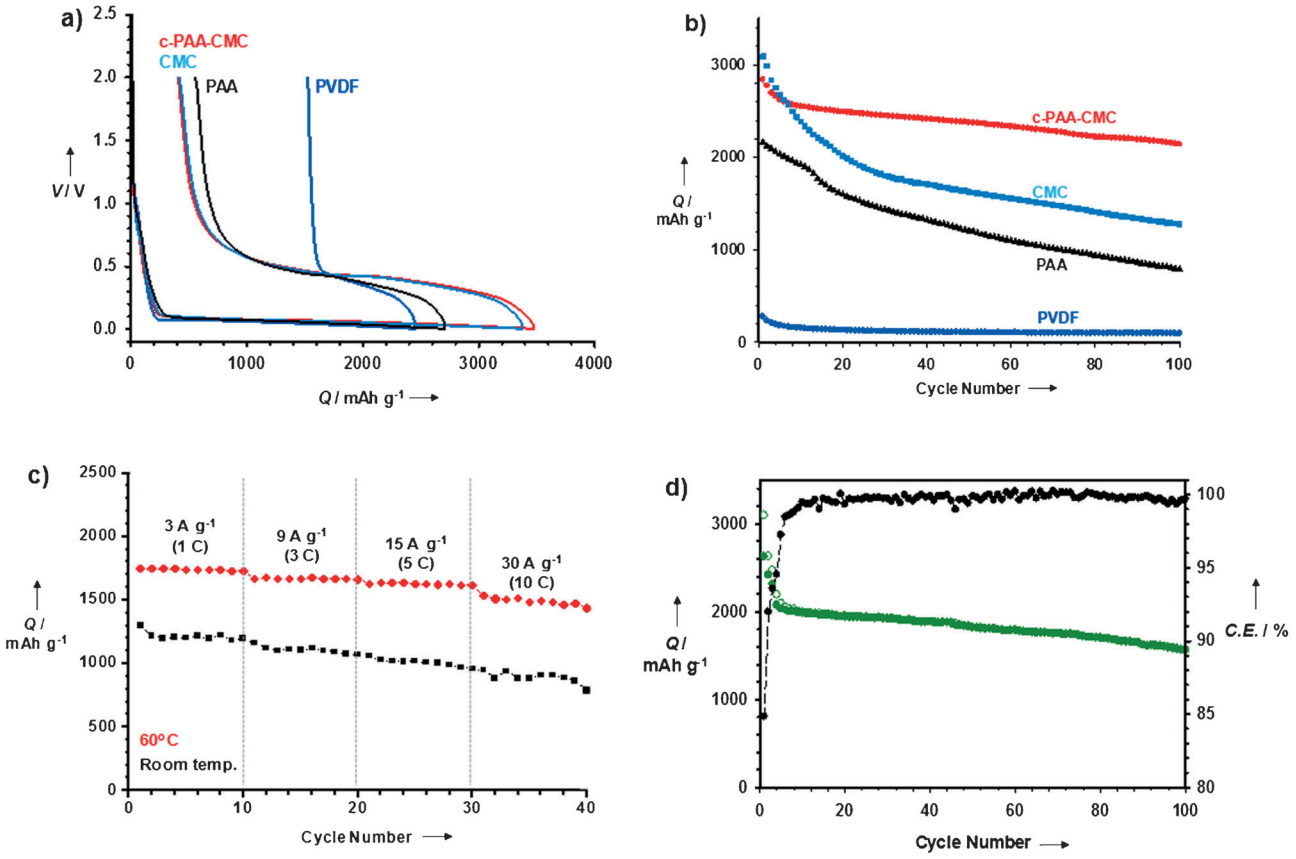

Figure 2. a) Initial charge–discharge profiles of silicon composite electrodes with thermally cured PAA-CMC (c-PAA-CMC), CMC, PAA, and PVDF binder at 175 $mA\,g^{-1}$ between 0.005 and 2.0 V versus Li/Li^+. b) Li extraction capacity versus cycle number for the silicon composite electrodes at a current density of 300 $mA\,g^{-1}$. c) Lithium extraction capacity of silicon anodes with c-PAA-CMC for various high current densities at room temperature and 60 °C. d) Specific capacity retention (green circle) of silicon composite anodes with c-PAA-CMC binder (electrode density = 0.4 $g\,cm^{-3}$) versus cycle number at a current density of 1500 $mA\,g^{-1}$ (corresponding to 0.5 C). A very high coulombic efficiency (black circles) of over 99.5%, which is vital for practical applications, was obtained during 100 cycles.

during cycling leads to degradation of the electrical conduction network, isolation of silicon nanoparticles, and finally capacity loss. Therefore, the difference in ICE stems from the mechanical properties of the binders. The silicon anode with PAA binder showed reduced capacities of 2705 and 2147 mAh g^{-1} for the first insertion and extraction of lithium, respectively (Figure 2a). This result indicates that bridges between the PAA binder and silicon nanoparticles are insufficient for preserving the electrical conductive network and hinder the electrochemical reaction of lithium with silicon nanoparticles during the insertion and extraction of lithium.[11a] In contrast, a significantly reduced irreversible capacity in the first cycle and improved long-term cycling performance were clearly observed for the silicon anodes with c-PAA-CMC binder (Figure 2a,b). The high value of the coulombic efficiency (88%) in the first cycle can be explained by several reasons.

First, the formation of covalent bonds between the silicon nanoparticles and c-PAA-CMC binder inhibits irreversible movement of silicon particles and keeps electrical contact between silicon and carbon black during the lithiation/delithiation process (Supporting Information, Figure S2). Second, the elimination of hydroxy (silanol and germinal groups of the SiO_2 layer on the silicon nanoparticles alleviates capacity loss by electrochemical reaction with lithium and contributes to the high coulombic efficiency (Supporting Information, Figure S2). Third, the cross-linked architecture of the binder allows the silicon nanoparticles to effectually utilize internal pores within the electrode with moderate volume expansion of the electrode during lithium insertion (Supporting Information, Figure S3). The first lithium extraction capacity obtained in a silicon anode with a linear-type CMC binder decreased slightly to 2955 mAh g^{-1}, giving an initial coulombic efficiency of 87.5% comparable with c-PAA-CMC binder. This is because the rigidity of CMC binder helps to mitigate volume expansion of the silicon anode.

Fluoroethylene carbonate (FEC) as a reducible additive is responsible for the formation of stable solid electrolyte interphase (SEI) on the silicon surface along with CMC binder.[17] Although CMC binder with the FEC-containing electrolyte provides high reversible capacity in the first cycle, the capacity gradually fades in subsequent cycles (Figure 2b). This result is in good agreement with the previous report that CMC binder cannot maintain the stable SEI during cycling.[12] However, c-PAA-CMC binder significantly improved lithium extraction capacity retention during cycling (Figure 2b,d). This is probably because the ester (COO) and ether (C-O-C) groups of c-PAA-CMC binder anchored on silicon nanoparticles can assist ion transport to the silicon surface, and c-PAA-CMC binder can endure the stress caused by the expansion of silicon nanoparticles.[12] The XPS peak corresponding to COONa and COO of c-PAA-CMC binder at 289 eV was clearly shown even after the precycle and was hardly detected after 30 cycles owing to the presence of SEI on the silicon surface (Figure 3). The peaks attributed to the SEI did not discernibly change between 30 and 100 cycles, supporting good capacity retention of silicon anodes with c-PAA-CMC binder. This is in good agreement with high coulmobic efficiency of over 99.5% indicating no lithium consumption by the electrolyte and binder decomposition (Supporting Information, Figure S4). Furthermore, impedance measurements showed that the interfacial resistance of the silicon composite anode with c-PAA-CMC binder was not substantially increased after 100 cycles (Supporting Information, Figure S5). This indicates that c-PAA-CMC binder preserves efficient electronic and ionic transport pathways at the silicon–electrolyte interface by the assistance of c-PAA-CMC binder for stable SEI during cycling and thereby realizes very good capacity retention.

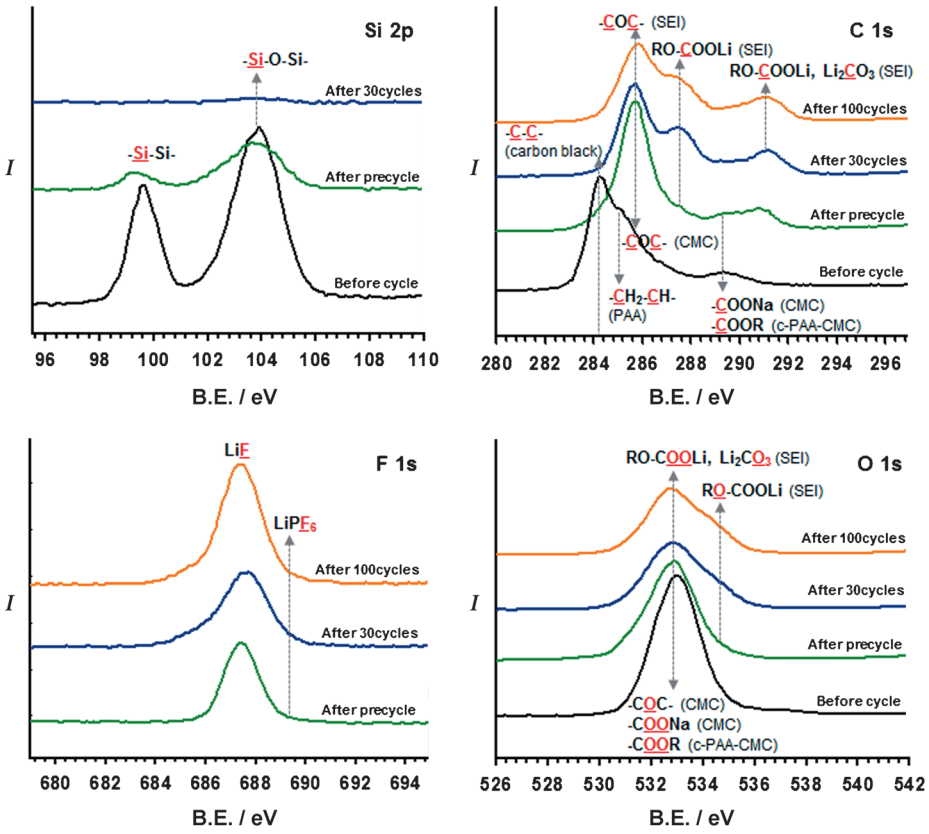

Figure 3. XPS spectra on the silicon anode surface with c-PAA-CMC binder before and after cycling between 0.005 and 2.0 V versus Li/Li$^+$. No peak corresponding to silicon indicates that the SEI formed by the electrolyte decomposition mostly covers the silicon nanoparticles after 30 cycles. The Si-O-Si peak at 103.8 eV is originated from an amorphous SiO_2 layer on the silicon nanoparticles.

To confirm that the c-PAA-CMC binder is robust enough for mechanical and electrical support, lithium extraction capacities were investigated for high current density (Figure 2c; Supporting Information, Figure S6a). We found that c-PAA-CMC binder retained high lithium extraction capacities of 850 mAh g^{-1} at room temperature and 1600 mAh g^{-1} at 60 °C for a very high current density of 30 A g^{-1} (corresponding to 10 C). However, sodium alginate binder with reactive hydroxy groups exhibited considerable capacity fading for the current density of 30 A g^{-1} at 60 °C (Supporting Information, Figure S6b). This is attributed to the formation of a resistive layer and the reduction of charge carrier concentration by the reaction between hydroxy groups and PF_5 from $LiPF_6$ ($LiPF_6 \leftrightarrow LiF + PF_5$). The lithium extraction capacity of the anode with sodium alginate binder 3037 mAh g^{-1} was comparable with that of to the anode with c-PAA-CMC binder (3063 mAh g^{-1}). However, the former had a lower initial coulombic efficiency (ICE) of 81 % compared with the latter (ICE = 88 %; Figure 2a; Supporting Information, Figure S6c). The lower ICE reflects the undesirable decomposition of hydroxy groups in the sodium alginate binder, which contributes to the irreversible capacity during first charge–discharge processes. Elimination of functional moieties, such as hydroxy and carboxylic acid, from polymeric binders is strictly required to assure good electrochemical performances of electrodes in LIB. Typical loading curves for the binder films without silicon nanoparticles and carbon black were obtained to compare the resistance of polymeric binders (PAA, CMC, c-PAA-CMC, and sodium alginate) to distort under mechanical load (Supporting Information, Figure S7). Even though c-PAA-CMC contains PAA with the lowest resistance to mechanical load, c-PAA-CMC binder showed relatively higher applied force for the same indentation depth compared to other linear polymers. CMC presented analogous resistance to mechanical load compared to c-PAA-CMC. This is closely linked to similar charge and discharge capacities during the precycle (Figure 2a). However, from the result of the capacity fading of silicon anode with CMC binder, it was confirmed that CMC is insufficient to endure repeated mechanical stress produced by the volume expansion of silicon nanoparticles during cycling (Figure 2b).

The thickness variation of silicon composite electrodes was measured to evaluate the ability of the binder to accommodate the large volume changes upon lithium insertion and extraction. The use of PVDF binder led to considerable volume expansion of about 130 % (Figure 4b; Supporting Information, Figure S8), whereas c-PAA-CMC binder better accommodated the expansional strain of silicon and thereby a drastically reduced thickness change of 35 % was obtained in the fully lithiated state (Figure 4a). The contribution of carbon black to the overall thickness change of silicon electrodes is negligible.[7c] The anode with PVDF binder did not reduce in thickness even after lithium extraction. During the discharging process, the expanded silicon nanoparticles shrink as lithium is extracted, but the final thickness of the electrode is still greater than original. This indicates that PVDF polymer cannot endure the internal stress and undergoes plastic deformation during lithium insertion. In contrast, the anode with c-PAA-CMC binder

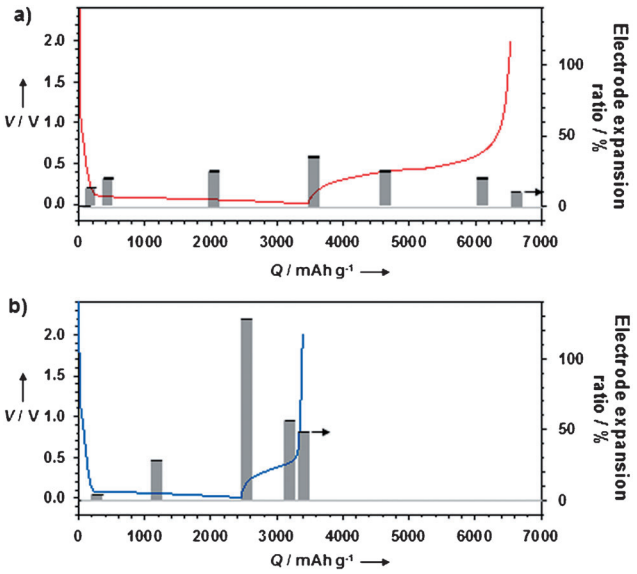

Figure 4. Charge–discharge profiles of a) c-PAA-CMC binder (red line) and b) PVDF binder (blue line). 2016 coin-type half cells were cycled for the current density of 175 mA g^{-1} at 30 °C in the potential range of 0.005 to 2.0 V versus Li/Li^+. The black lines represent the electrode volume changes during Li insertion and extraction processes. The use of c-PAA-CMC binder better accommodated the expansional strain of silicon in the fully lithiated state compared to PVDF binder.

almost fully recovered its initial thickness after lithium extraction (Supporting Information, Figure S9). This is because c-PAA-CMC binder has a high mechanical strength representing resistance to permanent deformation. This provides evidence that c-PAA-CMC binder significantly tolerates the internal mechanical stresses generated by the volume expansion of silicon nanoparticles and alleviates the volume expansion during lithiation. It is thus strongly believed that the combination of well-developed nanostructured silicon anode materials and our binder system will achieve a practically acceptable volume change of about 10 %. Moreover, after winding silicon electrode with c-PAA-CMC, there was no discernible physical fracture (Supporting Information, Figure S10). It should be noted that c-PAA-CMC can be used as an appropriate binder for commercialized graphite anodes (Supporting Information, Figure S11).

In conclusion, we have demonstrated that a cross-linked binder comprising cyclic and linear polymers can be utilized to improve the cycling performance and mitigate the large volume expansion of silicon anodes upon lithium insertion. This innovative binder will provide a practical solution for silicon-based anodes, which are otherwise a very promising candidate electrode material. Furthermore, the cross-linked binder can be applied to silicon–graphite composite, silicon dioxide, and tin-based anodes for lithium ion batteries with high energy density.

Received: February 27, 2012
Revised: June 18, 2012
Published online: July 29, 2012

Keywords: anodes · binders · cross-linking · lithium ion batteries · silicon

[1] a) K. T. Lee, J. Cho, *Nano Today* **2011**, *6*, 28; b) H. S. Zhou, D. L. Li, M. Hibino, I. Honma, *Angew. Chem.* **2005**, *117*, 807 – 812; *Angew. Chem. Int. Ed.* **2005**, *44*, 797 – 802; c) A. S. Aricò, P. G. Bruce, B. Scrosati, J. M. Tarascon, W. van Schalkwijk, *Nat. Mater.* **2005**, *4*, 366 – 377; d) M.-K. Song, S. Park, F. M. Alamgir, J. Cho, M. Liu, *Mater. Sci. Eng. R* **2011**, *72*, 203 – 252; e) L.-F. Cui, R. Ruffo, C. K. Chan, H. Peng, Y. Cui, *Nano Lett.* **2009**, *9*, 491 – 495.

[2] a) Y.-S. Hu, R. Demir-Cakan, M.-M. Titirici, J.-O. Müller, R. Schlögl, M. Antonietti, J. Maier, *Angew. Chem.* **2008**, *120*, 1669 – 1673; *Angew. Chem. Int. Ed.* **2008**, *47*, 1645 – 1649; b) C. K. Chan, H. Peng, G. Liu, K. McIlwrath, X. F. Zhang, R. A. Huggins, Y. Cui, *Nat. Nanotechnol.* **2008**, *3*, 31 – 35.

[3] a) M. Yoshio, H. Wang, K. Fukuda, T. Umeno, N. Dimov, Z. Ogumi, *J. Electrochem. Soc.* **2002**, *149*, A1598 – A1603; b) T. D. Hatchard, J. R. Dahn, *J. Electrochem. Soc.* **2004**, *151*, A1628 – A1635.

[4] a) H. Kim, B. Han, J. Choo, J. Cho, *Angew. Chem.* **2008**, *120*, 10305 – 10308; *Angew. Chem. Int. Ed.* **2008**, *47*, 10151 – 10154; b) J. Cho, *J. Mater. Chem.* **2010**, *20*, 4009 – 4014.

[5] a) S.-H. Ng, J. Wang, D. Wexler, K. Konstantinov, Z.-P. Guo, H.-K. Liu, *Angew. Chem.* **2006**, *118*, 7050; *Angew. Chem. Int. Ed.* **2006**, *45*, 6896; b) R. Teki, M. K. Datta, R. Krishnan, T. C. Parker, T.-M. Lu, P. N. Kumta, N. Koratkar, *Small* **2009**, *5*, 2236 – 2242.

[6] J. H. Lee, H. M. Lee, S. Ahn, *J. Power Sources* **2003**, *119 – 121*, 833 – 837.

[7] a) H. P. Zhao, C. Y. Jiang, X. M. He, H. G. Ren, C. R. Wan, *J. Membr. Sci.* **2008**, *310*, 1 – 6; b) V. A. Sethuraman, K. Kowolik, V. Srinivasan, *J. Power Sources* **2011**, *196*, 393 – 398; c) S. D. Beattie, D. Larcher, M. Morcrette, B. Simon, J. M. Tarascon, *J. Electrochem. Soc.* **2008**, *155*, A158 – A163.

[8] C. Martin, M. Alias, F. Christien, O. Crosnier, D. Bélanger, T. Brousse, *Adv. Mater.* **2009**, *21*, 4735 – 4741.

[9] a) J. Li, R. B. Lewis, J. R. Dahn, *Electrochem. Solid-State Lett.* **2007**, *10*, A17 – A20; b) N.-S. Choi, K. H. Yew, W.-U. Choi, S.-S. Kim, *J. Power Sources* **2008**, *177*, 590 – 594.

[10] D. Guy, B. Lestriez, D. Guyomard, *Adv. Mater.* **2004**, *16*, 553 – 557.

[11] a) A. Magasinski, B. Zdyrko, I. Kovalenko, B. Hertzberg, R. Burtovyy, C. F. Huebner, T. F. Fuller, I. Luzinov, G. Yushin, *Appl. Mater. Inter.* **2010**, *2*, 3004 – 3010; b) H. Buqa, M. Holzapfel, F. Krumeich, C. Veit, P. Novak, *J. Power Sources* **2006**, *161*, 617 – 622; c) N. S. Hochgatterer, M. R. Schweiger, S. Koller, P. R. Raimann, T. Wöhrle, C. Wurm, M. Winter, *Electrochem. Solid-State Lett.* **2008**, *11*, A76 – A80; d) B. Lestriez, S. Bahri, I. Sandu, L. Roue, D. Guyomard, *Electrochem. Commun.* **2007**, *9*, 2801 – 2806.

[12] I. Kovalenko, B. Zdyrko, A. Magasinski, B. Hertzberg, Z. Milicev, R. Burtovyy, I. Luzinov, G. Yushin, *Science* **2011**, *334*, 75 – 79.

[13] C. L. Campion, W. Li, B. L. Lucht, *J. Electrochem. Soc.* **2005**, *152*, A2327 – A2334.

[14] K.-F. Arndt, A. Richter, S. Ludwig, J. Zimmermann, J. Kressler, D. Kuckling, H.-J. Adler, *Acta Polym.* **1999**, *50*, 383 – 390.

[15] L. Pajchel, P. Nykiel, W. Kolodziejski, *J. Pharm. Biomed. Anal.* **2011**, *56*, 846 – 850.

[16] J.-S. Bridel, T. Azaïs, M. Morcrette, J.-M. Tarascon, D. Larcher, *Chem. Mater.* **2010**, *22*, 1229 – 1241.

[17] a) V. Etacheri, O. Haik, Y. Goffer, G. A. Roberts, I. C. Stefan, R. Fasching, D. Aurbach, *Langmuir* **2012**, *28*, 965 – 976; b) N.-S. Choi, K. H. Yew, K. Y. Lee, M. Sung, H. Kim, S.-S. Kim, *J. Power Sources* **2006**, *161*, 1254 – 1259.

